4

Particle pair interactions

We have previously considered the disturbance flow and stress fields due to a single particle immersed in a flow at low Re. Results obtained in the previous chapters are essential to develop understanding and rationalize the behavior of suspensions. For example, these results provide immediate insight into the fact that hydrodynamic interactions of particles are long-ranged. Our purpose here is to move forward to consider the interactions of a pair of particles in a viscous fluid, and we will limit consideration to spheres. We will consider these interactions in the case of a sedimenting pair and of a pair subjected to shear flow; these are the basic elements of the development of a full theory of suspension mechanics where many interacting particles should be considered. The interactions of close pairs as well as widely separated pairs will be discussed in sufficient detail to allow the reader to understand the motion of a pair and the basis of many-particle simulation tools.

4.1 A sedimenting pair

We turn to the settling of a pair of spheres of radii a_1 and a_2 under the action of gravity in a quiescent fluid as shown in Figure 4.1. The dynamics is driven by the gravity forces acting on each sphere $\mathbf{F}_1^{\mathrm{e}} = 4\pi a_1^3(\rho_{\mathrm{p}} - \rho)\mathbf{g}/3$ and $\mathbf{F}_2^{\mathrm{e}} = 4\pi a_2^3(\rho_{\mathrm{p}} - \rho)\mathbf{g}/3$. Since we are again considering Stokes flow with no particle inertia, the drag force on each particle must balance the gravity force: $\mathbf{F}_1^{\mathrm{h}} + \mathbf{F}_1^{\mathrm{e}} = 0$ and $\mathbf{F}_2^{\mathrm{h}} + \mathbf{F}_2^{\mathrm{e}} = 0$.

At very large separation ($r \to \infty$), the particles do not interact at all. The motion of each sphere is determined by the Stokes law for an isolated sphere

https://doi.org/10.1017/CBO9780511894671.006 Published online by Cambridge University Press

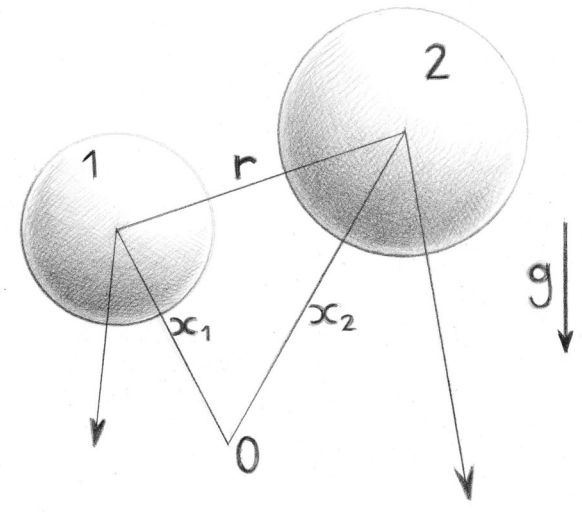

Figure 4.1 Sedimenting pair of spheres.

$$\mathbf{U}_1 = \frac{\mathbf{F}_1^{\mathrm{e}}}{6\pi\mu a_1} \quad \text{and} \quad \mathbf{U}_2 = \frac{\mathbf{F}_2^{\mathrm{e}}}{6\pi\mu a_2}. \tag{4.1}$$

These results, developed in Chapter 2, show the linearity of the relationship between forces and velocities. We can place these results in the general framework, developed in Chapter 3, of the mobility formulation,

$$\mathbf{U}_1 = \mathbf{M}_{11} \cdot \mathbf{F}_1^{\mathrm{e}} \quad \text{and} \quad \mathbf{U}_2 = \mathbf{M}_{22} \cdot \mathbf{F}_2^{\mathrm{e}}, \tag{4.2}$$

with $\mathbf{M}_{11} = \mathbf{I}/6\pi\mu a_1$ and $\mathbf{M}_{22} = \mathbf{I}/6\pi\mu a_2$. The separation must be very large for these results for isolated particles to hold because we know that the *fluid* velocity field induced by a sedimenting sphere decays very slowly as r^{-1}. If the separation is not so large, the particles interact hydrodynamically: the fluid motion induced by one particle will affect the motion of the other and vice versa. This interaction makes it appear that particle 2 responds to the force acting on particle 1 and vice versa. This leads us to write the above mobility formulation in a more general fashion

$$\begin{pmatrix} \mathbf{U}_1 \\ \mathbf{U}_2 \end{pmatrix} = \begin{pmatrix} \mathbf{M}_{11} & \mathbf{M}_{12} \\ \mathbf{M}_{21} & \mathbf{M}_{22} \end{pmatrix} \cdot \begin{pmatrix} \mathbf{F}_1^{\mathrm{e}} \\ \mathbf{F}_2^{\mathrm{e}} \end{pmatrix}. \tag{4.3}$$

We see again the linearity in the velocity response to the forces. Unlike the case of the single-particle problem, where the mobility tensor is

https://doi.org/10.1017/CBO9780511894671.006 Published online by Cambridge University Press

determined by only the shape and size of the particle and the fluid viscosity, the tensors $\mathbf{M}_{ij}$ depend also upon the separation vector between the particles. Hence, the mobility varies as the separation changes with the sedimentation process in the general case. Note that the off-diagonal tensors $\mathbf{M}_{12}$ and $\mathbf{M}_{21}$ are new quantities introduced by hydrodynamic interaction.

When we considered the single sphere motion in the previous chapters, we were able to compute the mobility or resistance tensors for that body. The question of interest now is to compute the mobility inclusive of pair interaction, and in particular to determine the tensors $\mathbf{M}_{ij}$ of equation (4.3). For moderate separation, the single-particle motion helps in deducing the behavior of the pair and this is done just below using an asymptotic method.

The method of reflections

We can first consider that the two spheres are far apart and thus their motion is determined by the Stokes drag law for an isolated sphere as we have seen before in (4.1):

$$\mathbf{U}_1^0 = \frac{\mathbf{F}_1^e}{6\pi\mu a_1} \quad \text{and} \quad \mathbf{U}_2^0 = \frac{\mathbf{F}_2^e}{6\pi\mu a_2}. \tag{4.4}$$

Here, the notation is slightly different with the superscript indicating that this is the lowest approximation, which we will call the zeroth reflection, as there is no interaction with the other particle. The method of reflections provides a systematic approach to improve upon this approximation to incorporate the hydrodynamic interactions.

Secondly, suppose that the spheres are only moderately far apart, in which case each affects the motion of the other. We will use the method of reflections, first used by Smoluchowski (1911) and described in great detail in chapter 6 of Happel and Brenner (1965) and in chapter 8 of Kim and Karrila (1989). The principle is to recognize that the velocity field created by sphere 1 (for instance) considered in isolation induces a velocity disturbance at the center of sphere 2 which causes sphere 2 to translate. Sphere 2 in turn will have an influence on sphere 1, and so on. Since the disturbance from sphere 1 interacting with the neighboring sphere 2 alters the motion and stress field of sphere 2, there is a "reflected" influence at sphere 1. It is this concept of reflected interactions which gives rise to the name of the method. This asymptotic technique is, of course, tedious if one wants to go up to higher reflections but the calculations

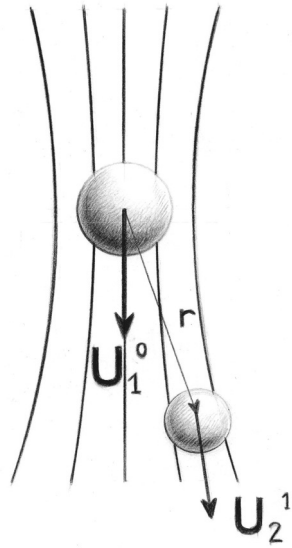

Figure 4.2 Method of reflection.

can be implemented numerically. For separations on the order of one particle radius or less, many reflections are needed for the method to be accurate; typically one resorts to other techniques, including lubrication theory which we will present in a following section.

To give just the flavor of the method, only the first reflection will be considered here. When no interactions are considered (zeroth reflection), the velocity of sphere 1 is given by $\mathbf{U}_1^0$. The motion of this sphere causes a fluid velocity disturbance

$$\mathbf{u}_1^0 = \left(\frac{\mathbf{I}}{r} + \frac{\mathbf{xx}}{r^3}\right) \cdot \frac{\mathbf{F}_1^{\mathrm{e}}}{8\pi\mu} + \left(\frac{\mathbf{I}}{3r^3} - \frac{\mathbf{xx}}{r^5}\right) \cdot \frac{a^2\mathbf{F}_1^{\mathrm{e}}}{8\pi\mu},$$

where $\mathbf{x}$ is the position vector with its origin at the center of sphere 1. Taking $\mathbf{x} = \mathbf{r}$ as shown in Figure 4.2, this disturbance causes the sphere 2 to translate with a first-reflection velocity given by the Faxén law for the force presented in Chapter 2,

$$\mathbf{U}_2^1 = \mathbf{u}_1^0(\mathbf{r}) + \frac{a_2^2}{6}\nabla^2\mathbf{u}_1^0(\mathbf{r}). \tag{4.5}$$

Note that this motion leaves the hydrodynamic force unchanged so $\mathbf{F}^{\mathrm{h}}$ continues to balance the gravity force $\mathbf{F}^{\mathrm{e}}$. Note also that $\mathbf{u}_1^0$ generates vorticity and thus, in order to remain torque-free, particle 2 must rotate. However, this does not affect the translation because there is

https://doi.org/10.1017/CBO9780511894671.006 Published online by Cambridge University Press

no translation–rotation coupling for the single sphere. The Laplacian term on the right hand side of this equation arises because sphere 2 is immersed in a flow $\mathbf{u}_1^0$ which is not linear. But if the spheres are widely separated, the $O(r^{-3})$ terms coming from the Laplacian can be neglected and the disturbance velocity $\mathbf{u}_1^0(\mathbf{r})$ created by sphere 1 at the center of sphere 2 is the remaining dominant term,

$$\mathbf{U}_2^1 = \frac{1}{8\pi\mu}\left(\frac{\mathbf{I}}{r} + \frac{\mathbf{rr}}{r^3}\right)\cdot\mathbf{F}_1^{\mathrm{e}} + O(r^{-3}). \tag{4.6}$$

To recover the total velocity of sphere 2, we use the linearity of the Stokes equations or to be more precise the principle of superposition by adding the zero-reflection velocity (sphere 2 in isolation submitted to an external force) and the first-reflection velocity (force-free sphere 2 immersed in the flow disturbance created by sphere 1),

$$\mathbf{U}_2^0 + \mathbf{U}_2^1 = \frac{\mathbf{I}}{6\pi\mu a_2}\cdot\mathbf{F}_2^{\mathrm{e}} + \frac{1}{8\pi\mu}\left(\frac{\mathbf{I}}{r} + \frac{\mathbf{rr}}{r^3}\right)\cdot\mathbf{F}_1^{\mathrm{e}} + O(r^{-3}). \tag{4.7}$$

We can proceed in the same manner to obtain the velocity of sphere 1 and finally we obtain the mobility relation with an error of $O(r^{-3})$:

$$\begin{pmatrix}\mathbf{U}_1\\ \mathbf{U}_2\end{pmatrix} = \begin{pmatrix}\frac{\mathbf{I}}{6\pi\mu a_1} & \frac{1}{8\pi\mu}\left(\frac{\mathbf{I}}{r} + \frac{\mathbf{rr}}{r^3}\right)\\ \frac{1}{8\pi\mu}\left(\frac{\mathbf{I}}{r} + \frac{\mathbf{rr}}{r^3}\right) & \frac{\mathbf{I}}{6\pi\mu a_2}\end{pmatrix}\cdot\begin{pmatrix}\mathbf{F}_1^e\\ \mathbf{F}_2^e\end{pmatrix}. \tag{4.8}$$

We are stopping at this first reflection but the reader should keep in mind that the process can be continued. It is interesting to note that, if the spheres are identical ($a_1 = a_2$, with each subject to the same external force), equation (4.8) shows that they fall at the same velocity and hence stay at constant distance apart. This result is true at any number of reflections and can also be deduced using only the principles of reversibility and superposition; see Exercise 1.2.

There are further consequences which can be readily obtained from equation (4.8) and which will be discussed further in the chapter on sedimentation. Since there is an additional component of the same sign along the direction of gravity, the first consequence is that another particle of any size causes a given particle to fall faster: two fall faster than one! Now considering spheres of the same size (although it is not necessary) we see that, in general, there is a component of motion which is not along the direction of gravity: two fall sideways at the same velocity! This sideways drift velocity decays to zero for large particle separation, i.e. for $r \to \infty$.

https://doi.org/10.1017/CBO9780511894671.006 Published online by Cambridge University Press

4.2 A pair in shear

We turn now to the case of a pair of spheres suspended in a shear flow, as illustrated for simple-shear flow by Figure 4.3. The ambient shear flow is given by $\mathbf{u}^\infty = (\dot{\gamma}y, 0, 0)$, which may be written $\mathbf{G}^\infty \cdot \mathbf{x} = (\mathbf{E}^\infty + \boldsymbol{\Omega}^\infty)\cdot\mathbf{x}$. The rotational portion of the motion, $\boldsymbol{\Omega}^\infty \cdot \mathbf{x}$, will be written below in terms of the rotational velocity of a material point in the undisturbed motion, $\boldsymbol{\omega}^\infty = \nabla \times \mathbf{u}^\infty/2$.

This problem differs from that of a sedimenting pair, in particular because the particle motions are driven here by the ambient fluid motion rather than by an external force. In fact, we are interested in the case of "freely suspended" particles, in which each particle has zero hydrodynamic force and torque. This requires that there are no interparticle forces (such as electrostatic forces) as well as a neutrally buoyant system, where the particles are of the same density as the fluid so that gravity does not affect the motion. The interesting feature of this problem is that the particles, despite being both force- and torque-free, deviate from their motions in isolation. The deviation results from their hydrodynamic interactions.

We first consider the isolated particle motions. As in the previous section, this implies consideration of a pair at large separation, $r \to \infty$. For a particle freely suspended in a shear flow, the requirements of vanishing force and torque immediately allow us to write – by making use of the Faxén laws given in Chapter 2 – the undisturbed motions as

$$\mathbf{U}_1^\infty = \mathbf{u}^\infty(\mathbf{x}_1), \quad \text{and} \quad \boldsymbol{\omega}_1^\infty = \boldsymbol{\omega}^\infty(\mathbf{x}_1), \tag{4.9}$$

$$\mathbf{U}_2^\infty = \mathbf{u}^\infty(\mathbf{x}_2), \quad \text{and} \quad \boldsymbol{\omega}_2^\infty = \boldsymbol{\omega}^\infty(\mathbf{x}_2). \tag{4.10}$$

Because the particles translate at the undisturbed velocity at their centers, the relative motion of a pair at large separation is given by

$$\mathbf{U}_{\mathrm{rel}} = \mathbf{U}_2^\infty - \mathbf{U}_1^\infty = \mathbf{G}^\infty \cdot (\mathbf{x}_2 - \mathbf{x}_1) = \mathbf{G}^\infty \cdot \mathbf{r}.$$

From this result, valid for arbitrary sphere sizes, we find that for certain separations the pair will move closer, while for others they will separate. This is easily seen by writing the result explicitly for simple-shear flow, where only the x-component of this "far-field" relative velocity is nonzero, $U_{\mathrm{rel},x} = \dot{\gamma}(y_2 - y_1)$. Hence, if $x_2 < x_1$ and $y_2 > y_1$, as shown in Figure 4.3, the pair approach one another as the result of the ambient motion.

https://doi.org/10.1017/CBO9780511894671.006 Published online by Cambridge University Press

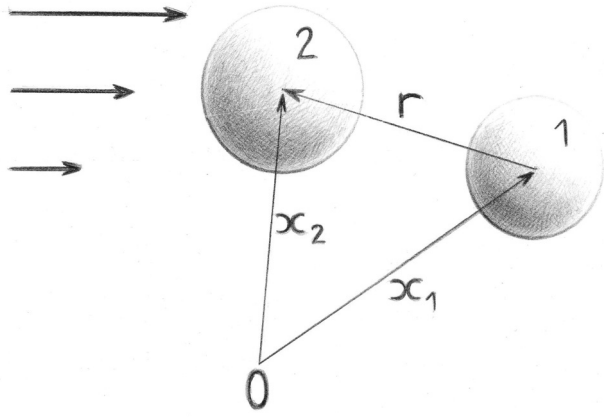

Figure 4.3 A pair of spheres in simple shear flow; x_1, x_2, and r in the drawing are vectors.

We now consider the particle velocity disturbances, i.e. $\mathbf{U}_i' = \mathbf{U}_i - \mathbf{U}_i^\infty$ for $i = 1$ or 2; we will limit consideration in the following to an equal-radius pair, $a = a_1 = a_2$. The disturbances occur for the same reason in shear flow as in the sedimentation problem of the previous section, specifically that the fluid disturbance flow caused by particle 1 influences particle 2 and vice versa. The particles deviate from the isolated-particle motions described by (4.9) and (4.10) in order to satisfy the requirement of remaining force- and torque-free. In Chapter 2, a particle immersed in a straining flow is shown to generate a disturbance flow owing to its non-deformability. The dominant effect is due to the stresslet (symmetric force dipole) exerted by the particle on the fluid. In the case of interest here, particle 2 causes a fluid velocity disturbance at the position of particle 1 of $\mathbf{u}(\mathbf{x}_1) - \mathbf{u}^\infty \sim r^{-2}$ owing to the stresslet-induced flow, where we recall that $\mathbf{x}_2 - \mathbf{x}_1 = \mathbf{r}$. In the terminology of the previous section, this leads to the first reflection approximation of the velocity of particle 1, $\mathbf{U}_1' = \mathbf{U}_1 - \mathbf{u}^\infty(\mathbf{x}_1) \sim r^{-2}$. For equal-sized particles, the symmetry of the pair-sphere problem leads directly to $\mathbf{U}_2' = -\mathbf{U}_1'$ at any separation.

With this physical basis for the particle disturbance velocities as a foundation, we now consider the problem using methods introduced in Chapter 3. We write the problem for the pair-sphere motion in the resistance formulation,

$$\begin{pmatrix} \mathbf{F}^{\mathrm{h}} \\ \mathbf{T}^{\mathrm{h}} \\ \mathbf{S}^{\mathrm{h}} \end{pmatrix} = \begin{pmatrix} \mathbf{0} \\ \mathbf{0} \\ \mathbf{S}^{\mathrm{h}} \end{pmatrix} = - \begin{pmatrix} \mathbf{R}^{\mathrm{FU}} & \mathbf{R}^{\mathrm{F}\omega} & \mathbf{R}^{\mathrm{FE}} \\ \mathbf{R}^{\mathrm{TU}} & \mathbf{R}^{\mathrm{T}\omega} & \mathbf{R}^{\mathrm{TE}} \\ \mathbf{R}^{\mathrm{SU}} & \mathbf{R}^{\mathrm{S}\boldsymbol{\omega}} & \mathbf{R}^{\mathrm{SE}} \end{pmatrix} \cdot \begin{pmatrix} \mathbf{U} - \mathbf{U}^{\infty} \\ \boldsymbol{\omega} - \boldsymbol{\omega}^{\infty} \\ -\mathbf{E}^{\infty} \end{pmatrix}, \tag{4.11}$$

where each vector accounts for both particles, e.g. $\mathbf{F}^{\mathrm{h}} = (\mathbf{F}^{\mathrm{h},1}, \mathbf{F}^{\mathrm{h},2})$, and the resistance tensors thus have both self- (11, 22) and interaction (12, 21) couplings.

Since both the force and torque are zero it proves convenient to further condense notation by writing

$$\begin{pmatrix} \hat{\mathbf{F}}^{\mathrm{h}} \\ \mathbf{S}^{\mathrm{h}} \end{pmatrix} = \begin{pmatrix} \mathbf{0} \\ \mathbf{S}^{\mathrm{h}} \end{pmatrix} = - \begin{pmatrix} \hat{\mathbf{R}}^{\mathrm{FU}} & \hat{\mathbf{R}}^{\mathrm{FE}} \\ \hat{\mathbf{R}}^{\mathrm{SU}} & \mathbf{R}^{\mathrm{SE}} \end{pmatrix} \cdot \begin{pmatrix} \hat{\mathbf{U}}' \\ -\mathbf{E}^{\infty} \end{pmatrix}, \tag{4.12}$$

where the hat (or caret) notation implies a combination of force and torque for $\hat{\mathbf{F}}^{\mathrm{h}} = (\mathbf{F}^{\mathrm{h}}, \mathbf{T}^{\mathrm{h}})$, of translational and rotational motion in $\hat{\mathbf{U}}' = (\mathbf{U} - \mathbf{U}^{\infty}, \boldsymbol{\omega} - \boldsymbol{\omega}^{\infty})$, and likewise a combination of translational and rotational couplings in the various resistance tensors. Note that the final row of (4.12), which gives the stresslets on the particles, is not necessary to compute the motions. However, in constructing the resistance matrix, all of the elements necessary for the stress calculation are determined, and it is natural to retain the square matrix. Now we expand the first row of the equation, to obtain

$$-\hat{\mathbf{R}}^{\mathrm{FU}} \cdot \hat{\mathbf{U}}' + \hat{\mathbf{R}}^{\mathrm{FE}} : \mathbf{E}^{\infty} = 0.$$

This equation may be solved for the velocities

$$\hat{\mathbf{U}}' = (\hat{\mathbf{R}}^{\mathrm{FU}})^{-1} \cdot \hat{\mathbf{R}}^{\mathrm{FE}} : \mathbf{E}^{\infty}. \tag{4.13}$$

Since the driving flow is known, and at a given pair separation the resistance tensors are also known, the pair motions are completely determined. The effort clearly comes in constructing and inverting the resistance tensors, but there is significant insight to be gained from this symbolic form. To begin, note that the equation can be interpreted as $\hat{\mathbf{U}}' = \hat{\mathbf{U}} - \hat{\mathbf{U}}^{\infty} = \hat{\mathbf{M}} \cdot \mathbf{F}^{\mathrm{E}}$, where $\hat{\mathbf{M}} = (\hat{\mathbf{R}}^{\mathbf{FU}})^{-1}$ is a translational-rotational mobility and $\mathbf{F}^{\mathrm{E}} = \hat{\mathbf{R}}^{\mathrm{FE}} : \mathbf{E}^{\infty}$ represents the forces (and torques) due to the interaction of the pair in a shear flow.

The interesting question arises: why is there a force associated with the pair motion in a straining flow? To understand the origin of the forces expressed as $\hat{\mathbf{R}}^{\mathrm{FE}} : \mathbf{E}^{\infty}$, imagine that the particles are immersed in a pure straining flow as depicted in Figure 4.4, so that $\mathbf{u}^{\infty} = \mathbf{E}^{\infty} \cdot \mathbf{x}$

https://doi.org/10.1017/CBO9780511894671.006 Published online by Cambridge University Press

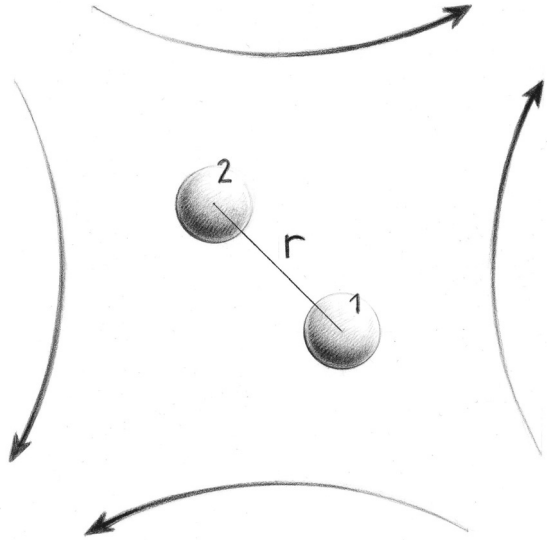

Figure 4.4 A pair of spheres in extensional flow.

and that the particles follow the bulk motion such that $\mathbf{U}_i = \mathbf{u}^\infty(\mathbf{x}_i)$ for particle i. Take the particles in a configuration aligned with the axis of compression, so that they simply approach one another with the ambient velocities at their centers. As the particle surfaces approach, each particle encounters the flow generated by the other as each pushes fluid in front of it. As a consequence, an elevated pressure is formed between the pair of particles, and the particles experience a hydrodynamic force which resists the relative motion, equal to $\hat{\mathbf{R}}^{\mathrm{FE}}{:}\mathbf{E}^\infty$. Note that this hypothetical particle motion cannot be imposed without an external force to balance the hydrodynamic force. This helps us to see that, in order that the hydrodynamic force and torque be zero, the particles must move with a velocity differing from the bulk motion such that

$$-\hat{\mathbf{R}}^{\mathrm{FU}}{\cdot}(\mathbf{U} - \mathbf{U}^\infty) + \hat{\mathbf{R}}^{\mathrm{FE}}{:}\mathbf{E}^\infty = 0. \tag{4.14}$$

Written in this way, the disturbance translational velocities are seen to be of just the magnitude necessary to obtain a zero hydrodynamic force. The vanishing hydrodynamic force itself appears as the sum of two canceling forces, each of which is hydrodynamic in origin. Of course, a similar argument could be made for the torque.

It is important to recall that, for an isolated sphere, $\mathbf{R}^{\mathrm{FE}} = 0$. Therefore if the pair is at very large separation, we expect to recover this result. At the same time, we recover $\mathbf{R}^{\mathrm{FU}} = 6\pi\mu a\mathbf{I}$ (for simplicity, we only consider translation and not rotation). Since, as we discussed previously, $\mathbf{U}_1' = \mathbf{U}_1 - \mathbf{u}^{\infty}(\mathbf{x}_1) \sim r^{-2}$ for particle 2 at a separation of r from particle 1, equation (4.14) implies that $\mathbf{R}^{\mathrm{FE}} \sim r^{-2}$. We see a similarity in the long-range interaction with the coupling between the particles in the sedimenting pair of the preceding section. The difference is that the decay is more rapid than the r^{-1} decay of the off-diagonal term of (4.8).

4.3 Pair lubrication interactions

Although it is a standard topic in fluid mechanics, having been developed by Reynolds (1886), the concept of lubrication, which arises when the separation between surfaces separated by fluid becomes small relative to the body size, is important enough that we will revisit the basic results here. We refer the reader to sources which treat the topic at different levels: chapter 4 of Ockendon and Ockendon (1995) provides an accessible introduction to the general topic, while chapter 9 of Kim and Karrila (1989) considers the specific geometry of interacting spheres. We consider here two spheres near contact with particular interest in the force required to impose the motion. More precisely, we consider two spheres (i) in relative translation along their line of centers (the squeeze flow problem) and (ii) in the plane perpendicular to this direction (the shear flow problem); see Figure 4.5. We will first simply state the results and give a simple physical basis for the difference seen in the force at the same separation distance in the two cases, and then turn to a more expanded analysis of the squeeze flow problem.

Figure 4.5 illustrates the physical situations in the two problems studied. In the squeeze flow problem, two spheres, that we choose for this discussion to be of the same radius a for simplicity, move along their line of centers with relative velocity $\mathbf{W}_{\mathrm{sq}}$. For the sake of concreteness, we consider the pair to be approaching one another and therefore squeezing the fluid out of the intervening gap which narrows with time. In the shear flow problem, the geometry is identical but the relative velocity $\mathbf{W}_{\mathrm{sh}}$ is perpendicular to the line of centers and therefore does not alter the width of the gap. In each case, we take a reference particle to be fixed and associate the relative motion with that of the other particle. The essential geometric feature of both problems is that the surface

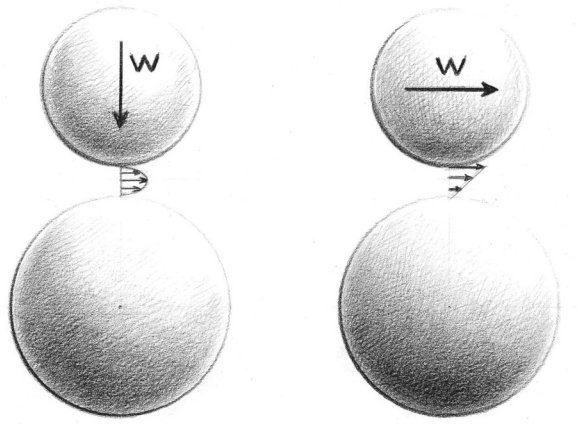

Figure 4.5 Squeezing and shearing problems.

separation $r - 2a = h_0 = \epsilon a$ is very small, i.e. $\epsilon \ll 1$. In either case, the force necessary to impose motion at the same speed W diverges as $\epsilon \to 0$ but the form of the divergence differs. In the squeeze flow problem, $F_{\text{sq}} \sim \mu a W \epsilon^{-1}$, while in the shear problem $F_{\text{sh}} \sim \mu a W \ln \epsilon$. To provide an order of magnitude, for a separation of 1% of a radius, or $\epsilon = 0.01$, the ratio $F_{\text{sq}}/F_{\text{sh}} \approx 50$.

Before turning to a mathematical discussion for the squeeze flow problem, we would like to provide some physical insight into the origin of the lubrication force. The basic idea is that the pressure in the gap becomes very large on a very small area surrounding the point of closest approach. In fact, $p \sim (\mu W/a)\epsilon^{-2}$ which is two factors of ϵ^{-1} larger than the flow-induced pressure surrounding the two spheres. Despite the fact that this large pressure acts on a very small area $S \sim \epsilon a^2$, the area is not small enough to avoid divergence, and thus $F_{\text{sq}} \sim pS \sim \mu a W \epsilon^{-1}$. It is important to note that if the relative motion is reversed so that the gap increases, an equally large negative pressure is developed so the magnitude of the force is the same but with the opposite sign. In other words, an increasing gap brings a negative pressure or suction while a decreasing gap generates a positive pressure. To illustrate this, note that in Figure 4.6, the gap in front of the moving particle (left sketch in the figure) is narrowed by the motion and the induced pressure is positive,

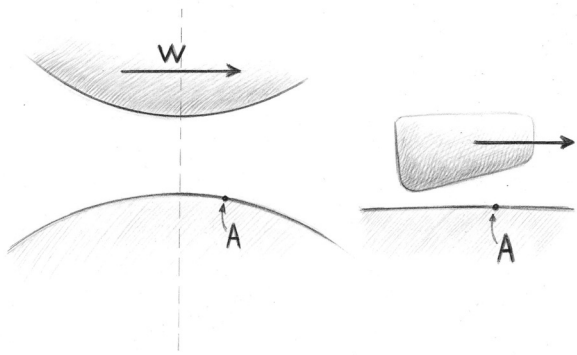

Figure 4.6 Blow-up of shearing and sliding block problems.

while the gap behind is increased and the induced pressure is negative. This is a result familiar to those who have encountered the classical sliding block problem solved by Reynolds (1886), also depicted in Figure 4.6 (right). Thus, a positive pressure is developed at the labeled point A in either case, but at the mirror image point of A for the spheres in the left portion of the figure, a negative pressure develops. These positive and negative pressures cancel in the vertical direction, normal to the motion. Considering the force in the direction of motion in this shearing problem, $p \sim (\mu W/a)\epsilon^{-2}$ as in the squeeze flow. However, the pressure acts only along the normal to the surface, which is almost vertical in the lubrication zone where this scaling of the pressure is valid. Hence, the component of the pressure force on the particle in the direction of tangential motion is quite small, thus reducing the strength of the force singularity. The logarithmic singularity requires a detailed consideration and the reader is referred to Leal (2007) and Kim and Karrila (1989).

Two spheres in squeeze flow

We consider the squeeze-flow problem in some detail for the more general case of two spheres of radii a_1 and a_2 approaching each other along their line of centers at relative velocity $\mathbf{W}$. We will give here the basic ingredients for solving the problem and computing the lubrication force. As the flow is axisymmetric, we will use cylindrical coordinates; see Figure 4.7. There are three basic steps in the argument.

https://doi.org/10.1017/CBO9780511894671.006 Published online by Cambridge University Press

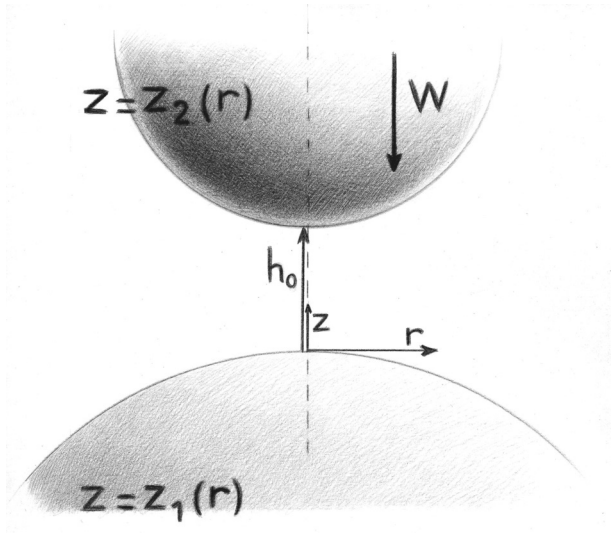

Figure 4.7 Squeezing problem with cylindrical geometry.

First, we approximate the spherical surfaces by paraboloids for small r. The distance between the sphere surfaces is then given by

$$h(r) = z_2 - z_1 \approx h_0 + \frac{r^2}{2}\left(\frac{1}{a_2} + \frac{1}{a_1}\right) = h_0\left(1 + \frac{r^2}{2ah_0}\right), \qquad (4.15)$$

where $a = a_1 a_2/(a_1 + a_2)$ is the reduced radius and $z_2(r)$ and $z_1(r)$ are the equations for the sphere surfaces. For the curvature term $r^2/2ah_0 = O(1)$, the radial r-length scale has to be $\sqrt{ah_0} = \epsilon^{1/2}a$ while the axial z-length scale is simply given by $h_0 = \epsilon a$.

Secondly, we consider the lubrication approximation. The basis of this theory is that, as the gap is very small $h_0 \ll a$ or $\epsilon \ll 1$, the axial z-length scale is much smaller than the radial r-length scale and that therefore the axial z-velocity scale is much smaller than the radial r-velocity scale. This can be ascertained by writing the continuity equation and deducing the appropriate velocity scales. The continuity equation is written as

$$\frac{1}{r}\frac{\partial(ru)}{\partial r} + \frac{\partial w}{\partial z} = 0, \qquad (4.16)$$

where u is the radial velocity and w the axial velocity. The axial z-velocity scale is unambiguously W. For the two terms to be of the same order in the continuity equation, one must take a radial r-velocity scale $U = W\sqrt{a/h_0} = \epsilon^{-1/2}W \gg W$. The flow is thus approximately unidirec-

https://doi.org/10.1017/CBO9780511894671.006 Published online by Cambridge University Press

tional. Using again the difference in r and z scales, $\nabla^2 u$ in the r-component of the momentum equation reduces to the variation across the gap. Keeping this dominant term and balancing it with the pressure variation which pumps the fluid out of the gap, one obtains

$$-\frac{\partial p}{\partial r} + \mu \frac{\partial^2 u}{\partial z^2} = 0, \tag{4.17}$$

providing the scale for the pressure $\mu a W/h_0^2 = (\mu W/a)\epsilon^{-2}$ that we advertised earlier. Note that if one assumes that the order of magnitude of the pressure is smaller and discards it, one obtains a trivial solution: $\partial^2 u/\partial z^2 = 0$ with $u = 0$ at the boundaries. With this scale of the pressure, an analysis of the z-component of the momentum equation shows that $\partial p/\partial z$ is by far the largest term. This leads to what may seem surprising: the largest term cannot be balanced and therefore must vanish,

$$\frac{\partial p}{\partial z} = 0. \tag{4.18}$$

In other words, the pressure is constant across the gap and depends only on the radial coordinate, $p = p(r)$. Solving equation (4.17) subject to the no-slip boundary conditions on the sphere surfaces gives the familiar parabolic velocity profile

$$u(r, z) = \frac{1}{2\mu} \frac{dp}{dr} [z - z_1(r)][z - z_2(r)]. \tag{4.19}$$

We have used the information from equation (4.18) to replace $\partial p/\partial r$ by dp/dr.

The third step is to satisfy the conservation of mass by requiring that the flux of fluid squeezed out over any radius be equal to the volume displaced by the moving spheres. This gives the pressure gradient which can be integrated once with respect to r with the zero pressure boundary condition at infinity to yield the expression for the pressure

$$p(r) = \frac{3\mu a W}{(h_0 + \frac{r^2}{2a})^2} = \frac{3\mu W/a}{\epsilon^2 (1 + \frac{r^2}{2a^2 \epsilon})^2}. \tag{4.20}$$

Note that allowing $r \to \infty$ simply means $r > O(\epsilon^{1/2} a)$. This pressure distribution shows that the pressure dominates the viscous stresses $|\mu \partial u/\partial z| = O(\mu W a^{1/2} h_0^{-3/2}) = O[(\mu W/a)\epsilon^{-3/2}]$, and is concentrated near the axis of symmetry. The magnitude of the lubrication force can

https://doi.org/10.1017/CBO9780511894671.006 Published online by Cambridge University Press

then be determined by integrating the pressure over the surface of either sphere

$$F^l = \int_{r=0}^{r\to\infty} p(r) 2\pi r dr = 6\pi\mu a^2 W/h_0 = 6\pi\mu a W \epsilon^{-1}. \tag{4.21}$$

The magnitude of the force is the same on each sphere but the directions are opposite as the forces are resisting the relative motion. For points on the sphere which are not close to the other sphere, the surface stress scales as $\mu W/a$ which would lead to a standard Stokes drag scaling as $\mu a W$. Therefore, neglect of the forces on the remainder of the sphere does not affect the leading result for the lubrication force.

As the lubrication force is inversely proportional to the small separation distance, it diverges as the spheres approach one another at a fixed relative velocity. Now if the imposed forces pushing the particles together are constant, the above equation can be written with $W = -dh_0/dt$,

$$F^l = -6\pi\mu a^2 \frac{dh_0}{dt}/h_0 \tag{4.22}$$

which can be solved to show that the spheres will approach each other exponentially slowly, i.e. $h_0(t) \sim \exp(-F^l t/6\pi\mu a^2)$.

Linearity again helps us, as the constant-force and constant-velocity problems are mathematically the same. This is made clearer by writing the lubrication force in a resistance formulation:

$$\begin{pmatrix} \mathbf{F}_1^{\mathrm{l}} \\ \mathbf{F}_2^{\mathrm{l}} \end{pmatrix} = -\boldsymbol{\mathcal{R}}^l \cdot \begin{pmatrix} \mathbf{U}_1 \\ \mathbf{U}_2 \end{pmatrix}, \tag{4.23}$$

with

$$\boldsymbol{\mathcal{R}}^l = \frac{6\pi\mu a^2}{h_0} \begin{pmatrix} 1 & -1 \\ -1 & 1 \end{pmatrix}.$$

This form of the resistance is specific to the squeeze flow problem but one can write a similar resistance matrix for the shear flow problem and obtain the complete lubrication description for general relative motion.

The above prediction of an infinite time before touching is a mathematical result which is valid only if the spheres are perfectly smooth. In reality, this is a good representation until the separation is comparable to the surface roughness and/or separation-dependent forces such as van der Waals attraction. These may lead to contact in a finite time. This has consequences for the collective properties of sheared suspensions, a topic that will be described in Chapter 7. Squeeze flow, which drives particles to very small separation, is a component of shear flow. The

fluid mechanical description of a pair motion is reversible in the Stokes regime but these non-hydrodynamic interactions associated with surface roughness and other forces introduce irreversibility.

4.4 Stokesian Dynamics

Stokesian Dynamics is a discrete-particle simulation technique for suspensions in Stokes flow. The method was developed by Bossis and Brady in the 1980s (see Brady and Bossis, 1988) and has been used and further developed extensively since. Stokesian Dynamics (SD) plays a role in the study of particles suspended in a viscous liquid similar to that which molecular dynamics (MD) plays for molecular gases and liquids. Rather than interacting strictly by conservative forces through vacuum as in MD, the discrete particles immersed in a viscous fluid, which is treated as a continuum, interact hydrodynamically. The hydrodynamic interactions are thus at the heart of the SD method, which we discuss in this chapter because it uses only *pair* hydrodynamic interactions to develop an approximate, but accurate, method for many-particle flow simulation.

The SD method is well-suited to rigid particles and has been applied primarily for suspensions of spherical particles. Because it allows inclusion of the effects of thermal (Brownian) motion of the particles, as well as the influence of interparticle and gravity forces, it may be applied across a wide range of conditions to model colloidal as well as non-colloidal dispersions in sedimentation and shearing flow.

Dynamic simulation methods compute the trajectories of the individual particles based on equations of motion, and from the resulting motion one may determine various properties of the system behavior. In a simulation of molecular dynamics, the equations of motion are familiar from Newtonian dynamics, e.g. for translational motion we have $\mathbf{F} = m\mathbf{a}$, where $\mathbf{F}$ is the net (or resultant) force on a particle, m is its mass, and $\mathbf{a} = d\mathbf{U}/dt$ is its acceleration. Typically, interest is in a many-body (say $N \gg 1$) system, and it is convenient to generalize this expression by taking $\mathbf{F} = (\mathbf{F}_1, \mathbf{F}_2, ..., \mathbf{F}_N)$ and similarly for the acceleration; if the masses of the particles vary, this can be accounted for by including them in the product $m\mathbf{a} \rightarrow (m_1\mathbf{a}_1, m_2\mathbf{a}_2, ..., m_N\mathbf{a}_N)$. Given a set of initial conditions for the particle positions and velocities, and a force law – usually of conservative form $\mathbf{F}_i = -\nabla_i V(\mathbf{x})$ where V is the potential energy of the N-body configuration $\mathbf{x}$ and ∇_i is a gradient with respect to the position of particle i – the equations of motion are

https://doi.org/10.1017/CBO9780511894671.006 Published online by Cambridge University Press

integrated to follow the evolution of the particle configuration with time, i.e. $\mathbf{x}(t) = \mathbf{x}(t=0) + \int_0^t \mathbf{U}(\tau)d\tau$.

The situation is similar for dynamic simulation of particles in viscous liquid. The equation of translational motion for the particles in the SD method comes from Newton's second law of motion and is the Langevin equation,

$$m\frac{d\mathbf{U}}{dt} = \mathbf{F}^{\mathrm{h}} + \mathbf{F}^{\mathrm{e}} + \mathbf{F}^{\mathrm{b}}, \tag{4.24}$$

where $\mathbf{F}^{\mathrm{h}}$ is the hydrodynamic force, $\mathbf{F}^{\mathrm{e}}$ represents both interparticle and external forces typically derivable from a potential, and $\mathbf{F}^{\mathrm{b}}$ is the random Brownian force representing the effect of a series of collisions with the molecules of the underlying fluid; we will provide a short discussion of Brownian motion in Chapter 5. As a result of the Brownian force, (4.24) is a stochastic differential equation, and some care must be taken in integrating this equation to properly account for the influence of thermal motion. For particles sufficiently large that Brownian motion may safely be neglected (roughly speaking above a few microns), the situation is simpler. For Stokes-flow conditions, the inertial term may be neglected and the non-Brownian particles obey

$$\mathbf{F}^{\mathrm{h}} + \mathbf{F}^{\mathrm{e}} = 0, \tag{4.25}$$

which is familiar from our analysis of sedimentation and other problems in previous chapters. This is the equation of motion for the particles: while the motion may seem to have disappeared from (4.25), it is implicit in the velocity dependence of the hydrodynamic term, $\mathbf{F}^{\mathrm{h}}$.

As it is necessary to describe the particle rotation as well as translation, we return to the notation defined above, where $\hat{\mathbf{F}}^{\mathrm{h}} = (\mathbf{F}^{\mathrm{h}}, \mathbf{T}^{\mathrm{h}})$, $\hat{\mathbf{U}} = (\mathbf{U}, \boldsymbol{\omega})$, and similarly we combine resistances involving translational and rotational couplings. The equation of motion for prescribed non-hydrodynamic forces and torques in a linear flow field can then be written as

$$-\hat{\mathbf{R}}^{\mathrm{FU}}\cdot(\hat{\mathbf{U}} - \hat{\mathbf{U}}^{\infty}) + \hat{\mathbf{R}}^{\mathrm{FE}}\!:\!\mathbf{E}^{\infty} + \hat{\mathbf{F}}^{\mathrm{e}} = 0, \tag{4.26}$$

where we have used the fact that the hydrodynamic forces and force moments are given by

$$\begin{pmatrix} \hat{\mathbf{F}} \\ \mathbf{S} \end{pmatrix} = -\boldsymbol{\mathcal{R}} \cdot \begin{pmatrix} \hat{\mathbf{U}} - \hat{\mathbf{U}}^{\infty} \\ -\mathbf{E}^{\infty} \end{pmatrix}, \quad \text{with} \quad \boldsymbol{\mathcal{R}} = \begin{pmatrix} \hat{\mathbf{R}}^{\mathrm{FU}} & \hat{\mathbf{R}}^{\mathrm{FE}} \\ \hat{\mathbf{R}}^{\mathrm{SU}} & \mathbf{R}^{\mathrm{SE}} \end{pmatrix}. \tag{4.27}$$

https://doi.org/10.1017/CBO9780511894671.006 Published online by Cambridge University Press

The equation may be solved formally for the particle motions

$$\hat{\mathbf{U}} - \hat{\mathbf{U}}^{\infty} = (\hat{\mathbf{R}}^{\mathrm{FU}})^{-1} \cdot (\hat{\mathbf{F}}^{\mathrm{e}} + \hat{\mathbf{R}}^{\mathrm{FE}} : \mathbf{E}^{\infty}). \tag{4.28}$$

Positions are updated using $\Delta\hat{\mathbf{x}} = \hat{\mathbf{U}}\Delta t$, where Δt is the computational time step; here $\hat{\mathbf{x}}$ includes the angular position. We note that the stresslets need not be computed to determine the particle motion: this mirrors the situation in MD, where the pressure is not needed to compute the motion but may be derived by post-processing of the particle positions and interparticle forces.

The primary computational effort of the SD method comes in computation of the grand resistance function $\boldsymbol{\mathcal{R}}$ for general many-body configurations. The essential concept which is used in the SD approach is that pair-sphere interactions can be described well by relatively simple forms at large separations (the far field) and at small separations (the near field). The two regions are handled quite differently, but it will be seen that the results of the previous sections of this chapter are sufficient to understand the concepts applied.

In the far field, the method of reflections can be used to develop an approximation of each of the mobilities making up the grand mobility $\boldsymbol{\mathcal{M}} = \boldsymbol{\mathcal{R}}^{-1}$ as a truncated series in r^{-1}. To make this point clearer, we recall that in the discussion of sedimentation in Section 4.1, the pair translational mobility was approximated to terms of $O(r^{-1})$ with an error of $O(r^{-3})$ in (4.8). At large r, a good approximation is obtained by truncation after a few terms in the series; tabulated coefficients are provided in, for example, chapter 11 of Kim and Karrila (1989). Because the series is truncated at a low order, the approximate grand mobility matrix is good only in the far field, and is termed $\boldsymbol{\mathcal{M}}^{\infty}$. An approximate form of the grand resistance matrix is obtained as $\boldsymbol{\mathcal{R}}^{\infty} = (\boldsymbol{\mathcal{M}}^{\infty})^{-1}$. For particles at surface separations comparable to their diameter, $\boldsymbol{\mathcal{R}}^{\infty}$ is a poor approximation, as the true behavior tends toward the singular lubrication behavior described in the previous section. Instead it is convenient to use the resistance functions obtained by lubrication analysis directly, $\boldsymbol{\mathcal{R}}^{l}$: these are intrinsically pair interactions because they arise from a local analysis in the gap between two particles. The grand resistance is constructed as

$$\boldsymbol{\mathcal{R}} = \boldsymbol{\mathcal{R}}^{\infty} + \boldsymbol{\mathcal{R}}^{l} - \boldsymbol{\mathcal{R}}^{l,\infty}. \tag{4.29}$$

We sum the near- and far-field approximations and subtract $\boldsymbol{\mathcal{R}}^{l,\infty}$, the part of the singular lubrication interaction captured by the inversion of the mobility matrix. The procedure is described in greater detail on page

128 of the review by Brady and Bossis (1988). This reference also points out that the far-field interactions change more slowly than the near-field interactions: clearly, r^{-1} for $r/a \geq O(1)$ is slowly varying relative to $(r-2a)^{-1}$ at $r-2a < O(1)$. For simulation of concentrated suspensions, this observation can be used to reduce the computational effort, as the mobility matrix and hence $\boldsymbol{\mathcal{R}}^{\infty}$ may be updated less frequently than the lubrication interactions $\boldsymbol{\mathcal{R}}^{l}$.

https://doi.org/10.1017/CBO9780511894671.006 Published online by Cambridge University Press